Hindawi
Journal of Nanotechnology
Volume 2021, Article ID 9401024, 7 pages
https://doi.org/10.1155/2021/9401024

Research Article

Synthesis of Cobalt-Nickel Nanoparticles via a Liquid-Phase Reduction Process

T. Usami,[1] S. A. Salman ,[2,3] K. Kuroda,[1] M. K. Gouda,[2] A. Mahdy,[2] and M. Okido[1]

[1]*Graduate School of Engineering Nagoya University, Nagoya, Japan*
[2]*Faculty of Engineering, Al-Azhar University, Cairo, Egypt*
[3]*Institute of Innovation for Future Society Nagoya University, Nagoya, Japan*

Correspondence should be addressed to S. A. Salman; sa.salman@yahoo.com

Received 10 August 2021; Revised 23 November 2021; Accepted 1 December 2021; Published 16 December 2021

Academic Editor: Brajesh Kumar

Cobalt-nickel nanoparticles (Co-Ni-NPs) show promising electrochemical performance in oxygen and hydrogen evolution reactions (OER and HER) due to their physicochemical properties such as electronic configuration and great electrochemical stability. Therefore, developing new economically and environmentally friendly methods of synthesizing Co-Ni-NPs has become a practical requirement. Co-Ni-NPs were produced by employing the liquid-phase reduction method. Nickel and cobalt sulfate solutions in hydrazine monohydrate with various mixing ratios were used as raw materials. Nickel plays an important role in the nucleation process via increasing the reduction reaction rate throughout the formation of Co-Ni-NPs. Furthermore, the acceleration of the Co-Ni-NPs formation process may be attributed to the partial dissolution of $Ni(OH)_2$ in the presence of N_2H_4 and/or citrate-anions and the formation of the Ni-N_2H_4 or Ni-Cit complexes in contrast to $Co(OH)_2$.

1. Introduction

Magnetic NPs have attracted increasing interest from researchers of many fields due to their promising applications in high-density magnetic storage media, magnetic refrigeration systems, ferrofluids, and biomedicine [1–3].

Nickel (Ni) and cobalt (Co) have attracted attention among the various magnetic NPs because of their excellent properties and industrial applications. The Ni-Co NPs are useful in many applications, including catalytic oxidation, hydrogenation, and hydrogen storage [4–8].

Electrochemical oxidation and reduction reactions, particularly the oxygen evolution reaction (OER) and hydrogen evolution reaction (HER), are the basis of various energy storage and conversion devices such as metal-air batteries, fuel cells, and water splitting to generate hydrogen and oxygen [9–12]. Electrocatalysts accelerate the kinetics for the electrochemical reactions by reducing the required overpotentials [13, 14]. The noble metal electrocatalysts, such as platinum for HER and ruthenium oxide for OER, showed excellent performance [15, 16]. However, because of the high cost and scarceness of these elements, searching for new alternatives is inevitable. Transition-metal-based materials, especially Co and Ni, are considered the most promising electrocatalysts for HER and OER due to their low cost and advanced catalytic performance comparable with the noble metals [11, 13, 16–19]. Therefore, it is advantageous to find a simple and cheap way to synthesize Co-Ni-NPs.

Several methods have been developed to synthesize magnetic NPs. Wet-chemistry methods are a powerful route for obtaining a reproducible macroscopic amount of a homogeneous specimen [20–23]. Liquid-phase reduction methods are relatively simple and do not require special equipment. Moreover, they are considered less expensive and quicker to implement, which are desirable qualities for future attempts at large-scale production [24–27]. Several colloidal chemical synthetic procedures have recently been developed to produce monodisperse NPs of magnetic materials [28–30].

Intensive research was done on the synthesis of Ni and Co in the presence of organic compounds such as ethanol and ethylene glycol [5, 31–35].

In previous research, Co NPs were successfully synthesized at room temperature by employing the liquid-phase reduction method and revealing the formation mechanism of particulates and the reaction mechanism of the reducing agent. Furthermore, the effect of citric acid additives on the shape and size of produced NPs was investigated [36–38].

In this study, Ni-Co NPs were fabricated in a solution that contained cobalt sulfate heptahydrate, nickel sulfate hexahydrate, and hydrazine monohydrate. Furthermore, the effect of the mixing ratio of nickel-based and cobalt-based solutions on the NPs was investigated.

2. Experimental Methods

2.1. Electrochemical Measurements. The electrochemical behaviors of Co and Ni in the experimental system were investigated using polarization measurements. Three electrodes cell of 1.0 cm^2 Ni and Co substrates with a purity of 99.9% as a working electrode. The counter and reference electrodes were Pt coils and Ag/AgCl sat. KCl, respectively.

The electrolyte for anodic polarization measurement comprises 1 M hydrazine monohydrate ($N_2H_4.H_2O$) and 0.2 M trisodium citrate dihydrate ($Na_3C_6H_5O_7.2H_2O$). All chemicals were dissolved in distilled water to make 200 ml of solution with an adjusted pH between 10 and 14.

The cathodic polarization measurements were performed in a solution of 0.1 M cobalt sulfate heptahydrate ($CoSO_4.7H_2O$) or 0.1 M nickel sulfate hexahydrate ($NiSO_4.6H_2O$), and 0.2 M trisodium citrate dihydrate ($Na_3C_6H_5O_7.2H_2O$). All chemicals were dissolved in distilled water to make 200 ml of solution adjusted to pH 14. The anodic and cathodic polarization were performed at 353 k and a scan rate of 1 mV S^{-1}.

2.2. Synthesis of Cobalt Nanoparticles. Cobalt sulfate heptahydrate ($CoSO_4.7H_2O$), nickel sulfate hexahydrate ($Ni_SO_4.6H_2O$), and hydrazine monohydrate ($N_2H_4.H_2O$) were used as raw materials.

The solution was prepared by adding an amount of 0.4 M trisodium citrate dihydrate ($Na_3C_6H_5O_7.2H_2O$) and 20 ml of citric acid to an aqueous solution of 50 to 80 M % of cobalt sulfate and 20 to 50 M % of nickel sulfate. These percentages were chosen because they are near the line boundary between ε (Co) and α (Co and Ni) in the Co-Ni phase diagram shown in Figure 1.

The pH of the solution was adjusted to 14 using 10 ml of 5 M sodium hydroxide (NaOH) and sulfuric acid. After adjusting the pH, 10 ml of 1 M hydrazine solution was added to the solution. The solution temperature was kept at 353 K, and the reaction time was 60–120 min, and the total amount of initial metal ions was adjusted to 0.2 M.

The solution used in the experiment was subjected to argon bubbling for 30 minutes before mixing to remove dissolved oxygen. The obtained precipitate was removed from the solvent by a centrifuge, washed several times with distilled water, and then dried using a vacuum dryer.

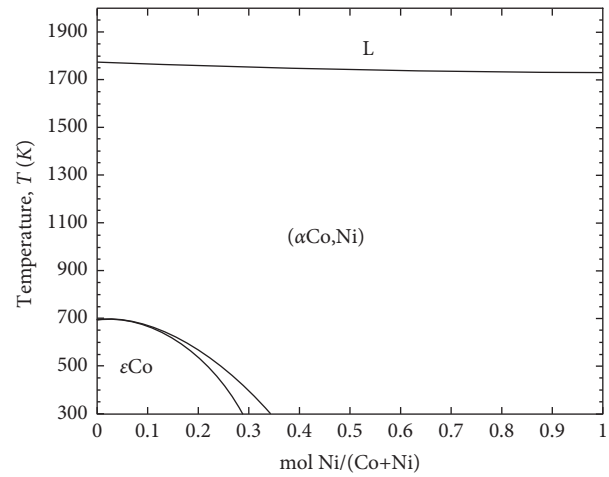

Figure 1: Co-Ni phase diagram (εCo, hcp. αCo, fcc, Ni. fcc).

The shapes and analysis of the NPs were observed with a scanning electron microscope (SEM) and energy dispersive spectroscopy (EDS). The phase structures were identified by employing X-ray diffraction (XRD). The chemical composition analysis was performed with the grain degree distribution measurement by inductively coupled plasma mass spectrometry (ICP-MS). Moreover, the mixed potential was measured while the reduction was reacted with a potentiostat equipped with a 1 cm^2 Co substrate and an Ag/AgCl sat. KCl reference electrode.

3. Results and Discussion

Figure 2 shows the potential pH diagram of Ni-H_2O and Co-H_2O. The figure shows that hydrazine can work effectively as a reducing agent since the oxidation potential of hydrazine is less noble than the reduction potential of both Co and Ni. Consequently, it is possible to synthesize Ni and Co NPs using hydrazine. Furthermore, the measured oxidation potential is similar to the Nernst equation's theoretical values (dashed line).

The cathodic polarization measurement is shown in Figure 3. This figure shows that it is easy to extract Co from cobalt solution; however, the extraction speed of Ni from Co solution seems to progress at a slower rate. The presence of montmorillonite NPs was likely precipitated on the working electrodes, reducing the active area of the working electrode metals in contact with the electrolyte leading to a decrease of cathodic current.

On the other hand, the extraction rate in the Ni solution is slower than in the Co solution. In other words, Ni^{2+} does not affect the growth of the particles; however, it may affect the nucleation process.

The noble metal salts such as Ag_2NO_3, $PdCl_2$, and H_2PtCl_6 are used as nucleating agents in the liquid-phase reduction method to form fine particles [39]. In the present study, it seems that the addition of Ni was found to have the same role as noble metals as a nucleating agent as well as phase change.

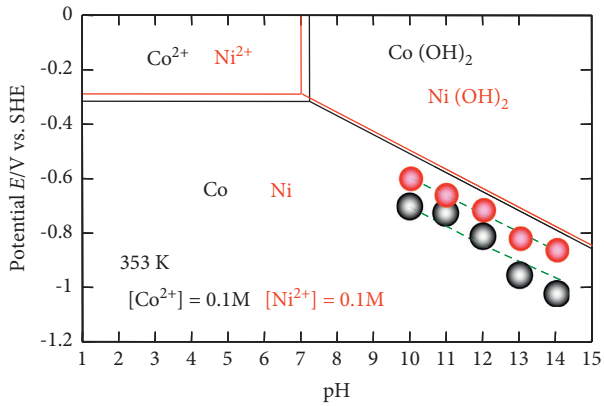

FIGURE 2: Potential pH diagram of the Co-H_2O and Ni–H_2O system and oxidation potential of hydrazine with citric acid additives.

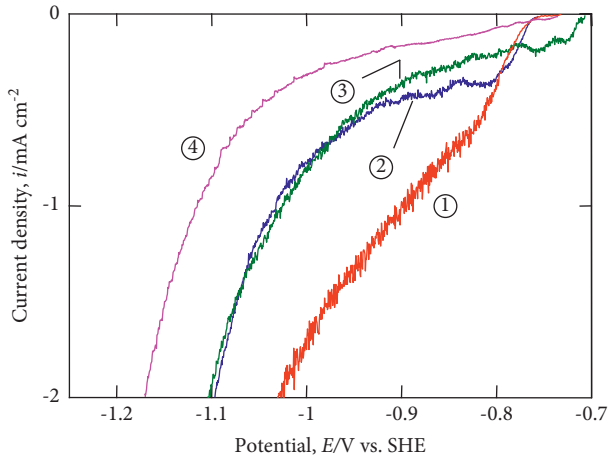

FIGURE 3: Cathode polarization measurements with WE: (1) Co in Co bath, (2) Ni in Co bath, (3) Ni in Ni bath, and (4) Co in Ni bath.

Figure 4 shows SEM images and a frequency histogram obtained by inductively coupled plasma mass spectrometry (ICP-MS) analysis of Co-Ni particles: (a) Co(II): Ni (II) = 2 : 8, (b) Co(II): Ni (II) = 5 : 5, and (c) Co(II): Ni (II) = 6 : 4 for the size range 1–10000 nm.

The Co-Ni-NPs showed a different size distribution of the semispherical shapes agglomerates. The lowest obtained NPs size were 50 nm at Co(II): Ni (II) = 2 : 8 molar ratio, 80 nm at Co(II) : Ni (II) = 6 : 4 molar ratio, and 350 nm at Co(II) : Ni (II) = 5 : 5 molar ratio. This agrees with Kytsya A.R et al. [25]; they reported that the nucleation rate of Ni-Co NPs is linearly increased with an increasing fraction of Ni in the reaction mixture. They also reported that the growth rate of the NPs increases up to the molar ratio of Co(II) : Ni (II) = 5 : 5. The nucleation of Ni-NPs occurs via partial dissolution of $Ni(OH)_2$ and formation on the surface of hydroxide particles of the complex Ni^{2+}-N_2H_4, which easily (EA~40 kJ/mol) decomposes, forming the nucleus of Ni-NPs.

The particles produced at Co(II) : Ni (II) = 5 : 5 molar ratio showed the highest degree of agglomeration compared to other lower and higher molar ratios. This is attributed to the adhesion of particles to each other by weak forces leading to submicron-sized entities. Various aggregates were measured as one particle in the dynamic particle size distribution measurement because dispersants were not used in these experiments.

The XRD analysis of the precipitates after 60 minutes of stirring is shown in Figure 5. The peaks of Ni (fcc) and αCo (fcc) were observed in all mixing ratios. At the mixing ratio of Co(II) : Ni (II) = 5 : 5, new peaks of $Ni(OH)_2$ and $Co(OH)_2$ were detected. This means that it was not possible to synthesize highly dispersible Co-Ni-NPs. It is considered that this is because the dispersant capped the precursors' $Co(OH)_2$ and Ni $(OH)_2$could not efficiently elute Co^{2+} and Ni^{2+}. These results are in good agreement with the Co-Ni phase diagram shown in Figure 1.

An ICP technique was conducted for the compositional analysis of all samples. The ICP allowed an accurate quantification of the Co and Ni content in the NPs. This also allowed us to measure the transferability of the precursor into the final product. The results are shown in Table 1.

The molar fraction of Ni is higher than that of the condition set in an initial solution in FCC particles. However, in the higher concentrations of Co, the molar fraction of Co increased in the HCP particles with an agreement with the Co-Ni phase diagram shown previously in Figure 1.

The reduction of Ni ions is thought to proceed according to the following reactions: in the first step, nickel(II) sulfate reacts with sodium hydroxide to produce nickel(II) hydroxide and sodium sulfate, as shown in the following equation:

$$NiSO_4 + 2NaOH \longrightarrow Ni(OH)_2\downarrow + Na_2SO_4 \quad (1)$$

In the second step, a chemical reduction process of the Ni ion with hydrazine as a reductant in an alkaline aqueous solution can proceed, as shown in the following equation:

$$2Ni(OH)_4 + N_2H_4 \longrightarrow 2Ni\downarrow + N_2\uparrow + 4H_2O \quad (2)$$

The dissociation of $Ni(OH)_2$ is considered the starting point of the reduction reaction, and it is affected by the reaction rate. There is no change in the pH of the solution according to the deposition of the metal cathode. The reduction reaction of Ni is being advanced by dissociating the nickel hydroxide to Ni^{2+}. Hydrazine is a highly reactive reducing agent in the alkaline medium; it acts more strongly as a reducing agent at high pH values [6].

The large and low numbers of the NPs agglomerates were formed at a higher molar concentration of NaOH. This agrees with Irfan et al. [26]. They reported that the size and number of the NPs agglomerates depend on the molar concentration of NaOH in the $NiSO_4$ solution. At low pH, the reduction rate of Ni ions becomes slow. The clusters become larger, and the NP agglomerates decrease when the molar concentration of NaOH is higher than 1 M.

The citric acid reacts with Ni^{2+} to form Ni^{2+}-citrate complexes, as shown in equation (3). It was reported that the proportion of Ni^{2+} to the citrate precipitated depends on its initial concentration and pH value [40, 41].

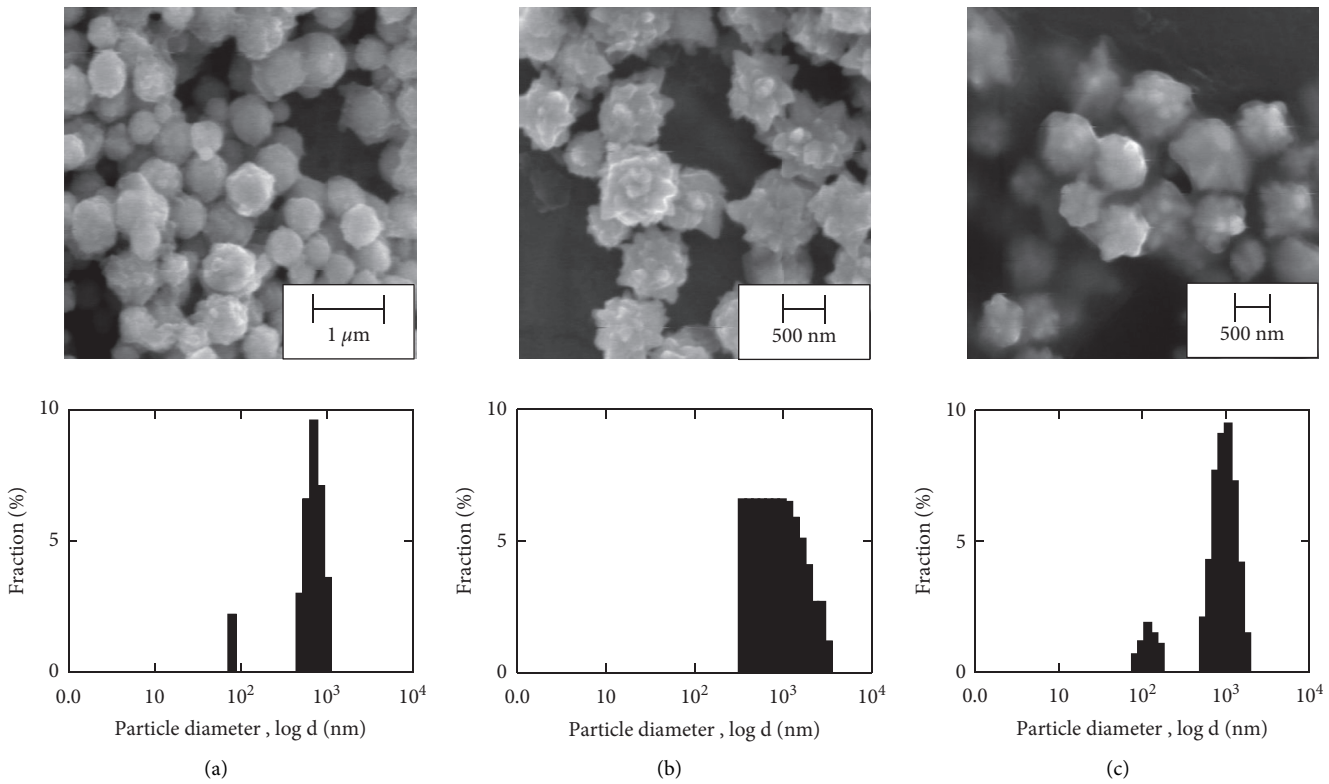

Figure 4: SEM images and a frequency histogram obtained by inductively coupled plasma mass spectrometry (ICP-MS) analysis of Co-Ni particles. (a) Co(II): Ni (II) = 2 : 8, (b) Co(II): Ni (II) = 5 : 5, and (c) Co(II): Ni (II) = 6 : 4.

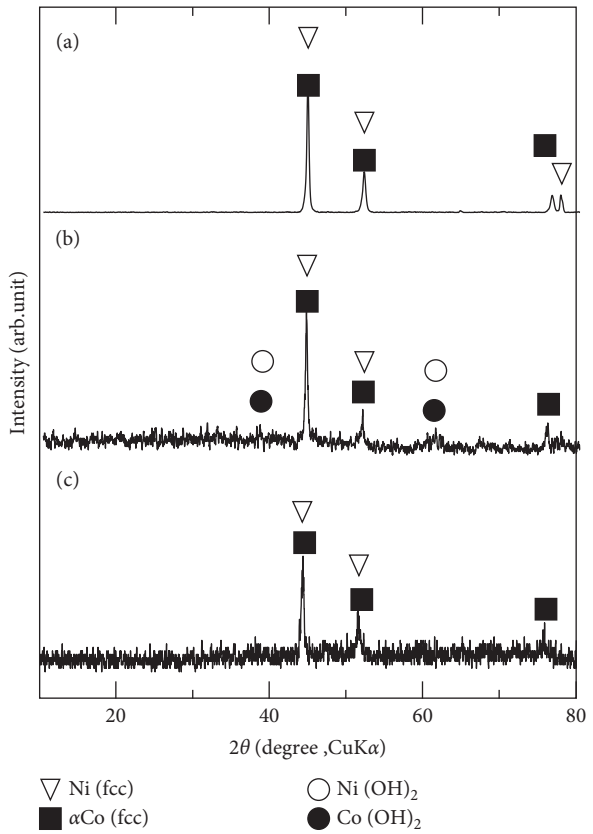

Figure 5: XRD analysis of Co-Ni particles. (a) Co(II): Ni (II) = 2 : 8, (b) Co(II): Ni (II) = 5 : 5, and (c) Co(II): Ni (II) = 6 : 4.

Table 1: ICP compositional analysis of produced nanoparticles.

Initial aqueous solution Co(II) : Ni(II)	The atomic ratio of metal in the particles Co : Ni
2 : 8	19.0 : 81.0
5 : 5	47.6 : 52.4
6 : 4	59.0 : 41.0

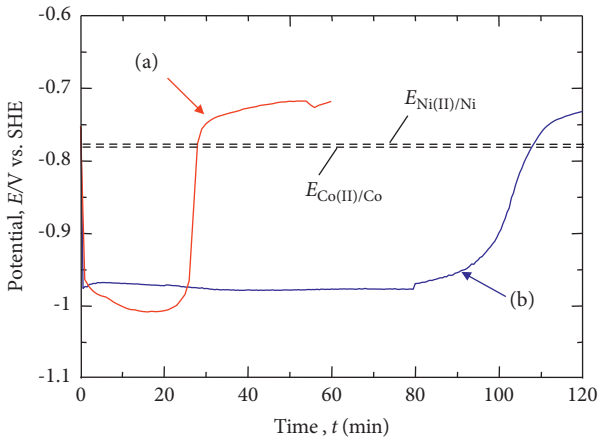

Figure 6: Mixed potential change and reduction potential of cobalt. (a) Co(II) : Ni(II) = 5 : 5 and (b) Co(II) : Ni(II) = 8 : 2.

$$Ni^{2+} + 2C_6H_5O_7^{3-} \longrightarrow Ni\left(C_6H_5O_7\right)_2^{4-} \quad (3)$$

The oxidation potential does not change with the addition of citric acid to the cobalt-hydrazine solution, which indicates that cobalt cannot form the complex compounds with hydrazine. Thus, $Co(OH)_2$ does not dissolve due to the high redox potential of the half-reaction.

$Co(OH)_2 + 2e^- \longrightarrow Co + 2OH^-$ ($E^0 = -0.73$ V) does not participate in the nucleation process. That is why the rate of nucleation linearly depends on the initial concentration of Ni^{2+}; we hypothesize that these nickel NPs act as active catalytic sites. The reduction reaction was progressed by adding trisodium citrate dihydrate to the cobalt-hydrazine solution [23].

Figure 6 shows the potential curves in the solution containing (a) Co: Ni = 5 : 5 and (b) Co: Ni = 8 : 2 during the reaction. After mixing the reductants, the potential dropped to −970 mV. Both lines rose very quickly after 22 min and 80 min, respectively. Many bubbles that were supposed to be N_2 have been observed during the increase of the potential. Then, the solution turned black, due to the formation of Co-Ni particles. The potential of E $Co/Co(OH)_2$ was very close to the theoretical equilibrium potential value (−785 mV). The curve showed that the potential was about −750 mV, with a difference of 35 mV from the theoretical value. The reaction effectively proceeds after the quick increase of the potential.

4. Conclusion

We investigated the synthesis and formation mechanism of Co-Ni-NPs using the liquid-phase reduction method. The phase structure was identified as Ni (fcc), αCo (fcc), and depends on the Co: Ni ratio variation. The oxidation potential does not change with the addition of citric acid to the cobalt-hydrazine solution, which means that cobalt hydroxide does not participate in the nucleation process. The rate of nucleation linearly depends on the initial concentration of Ni^{2+} in the reaction mixture. The lowest obtained NP sizes were 50 nm at Co(II): Ni (II) = 2 : 8 molar ratio, 80 nm at Co(II): Ni (II) = 6 : 4 molar ratio, and 350 nm at Co(II): Ni (II) = 5 : 5 molar ratio.

Data Availability

The data that support the findings of this study are available from the corresponding author on reasonable request.

Conflicts of Interest

The authors declare that they have no conflicts of interest.

Acknowledgments

The authors gratefully acknowledge the Ministry of Higher Education of the Arab Republic of Egypt and the Ministry of Education, Culture, Sports, Science and Technology of Japan.

References

[1] A. F. Khusnuriyalova, M. Caporali, E. Hey-Hawkins, O. G. Sinyashin, and D. G. Yakhvarov, "Preparation of cobalt nanoparticles," *European Journal of Inorganic Chemistry*, vol. 2021, no. 30, pp. 3023–3047, 2021.

[2] Z. Zhang, X. Chen, X. Zhang, and C. Shi, "Synthesis and magnetic properties of nickel and cobalt nanoparticles obtained in DMF solution," *Solid State Communications*, vol. 139, no. 8, pp. 403–405, 2006.

[3] M. D. J. Ooi, A. A. Aziz, and R. Adnan, "Solvent effects on the structural and catalytic properties of Pt nano- and microstructures synthesised in solvothermal system," *International Journal of Hydrogen Energy*, vol. 46, no. 8, pp. 5926–5937, 2021.

[4] Y. G. Morozov, O. V. Belousova, and M. V. Kuznetsov, "Preparation of nickel nanoparticles for catalytic applications," *Inorganic Materials*, vol. 47, no. 1, pp. 36–40, 2011.

[5] S. Schrittwieser, D. Reichinger, and J. Schotter, "Applications, surface modification and functionalization of nickel nanorods," *Materials*, vol. 11, no. 1, 2018.

[6] L. He, H. Berntsen, E. Ochoa-Fernández, J. C. Walmsley, E. A. Blekkan, and D. Chen, "Co-Ni catalysts derived from hydrotalcite-like materials for hydrogen production by ethanol steam reforming," *Topics in Catalysis*, vol. 52, no. 3, pp. 206–217, 2009.

[7] X. Huang, X. Xiao, W. Zhang et al., "Transition metal (Co, Ni) nanoparticles wrapped with carbon and their superior catalytic activities for the reversible hydrogen storage of magnesium hydride," *Physical Chemistry Chemical Physics*, vol. 19, no. 5, pp. 4019–4029, 2017.

[8] Y. Zhu, X. Zhong, X. Jia, and J. Yao, "Bimetallic Ni-Co nanoparticles confined within nitrogen defective carbon nitride nanotubes for enhanced photocatalytic hydrogen production," *Environmental Research*, vol. 203, p. 111844, 2022.

[9] M. Tahir, L. Pan, F. Idrees et al., "Electrocatalytic oxygen evolution reaction for energy conversion and storage: a

comprehensive review," *Nanomaterials and Energy*, vol. 37, pp. 136–157, 2017.

[10] Z.-L. Wang, D. Xu, J.-J. Xu, and X.-B. Zhang, "Oxygen electrocatalysts in metal-air batteries: from aqueous to non-aqueous electrolytes," *Chemical Society Reviews*, vol. 43, no. 22, pp. 7746–7786, 2014.

[11] Y. Yan, B. Y. Xia, B. Zhao, and X. Wang, "A review on noble-metal-free bifunctional heterogeneous catalysts for overall electrochemical water splitting," *Journal of Materials Chemistry*, vol. 4, no. 45, pp. 17587–17603, 2016.

[12] H.-F. Wang, L. Chen, H. Pang, S. Kaskel, and Q. Xu, "MOF-derived electrocatalysts for oxygen reduction, oxygen evolution and hydrogen evolution reactions," *Chemical Society Reviews*, vol. 49, no. 5, pp. 1414–1448, 2020.

[13] D. Li, J. Shi, and C. Li, "Transition-metal-based electrocatalysts as cocatalysts for photoelectrochemical water splitting: a mini review," *Small*, vol. 14, no. 23, p. 1704179, 2018.

[14] C. C. L. McCrory, S. Jung, I. M. Ferrer, S. M. Chatman, J. C. Peters, and T. F. Jaramillo, "Benchmarking hydrogen evolving reaction and oxygen evolving reaction electrocatalysts for solar water splitting devices," *Journal of the American Chemical Society*, vol. 137, no. 13, pp. 4347–4357, 2015.

[15] Y. Jiao, Y. Zheng, M. Jaroniec, and S. Z. Qiao, "Design of electrocatalysts for oxygen- and hydrogen-involving energy conversion reactions," *Chemical Society Reviews*, vol. 44, no. 8, pp. 2060–2086, 2015.

[16] M. S. Burke, L. J. Enman, A. S. Batchellor, S. Zou, and S. W. Boettcher, "Oxygen evolution reaction electrocatalysis on transition metal oxides and (Oxy)hydroxides: activity trends and design principles," *Chemistry of Materials*, vol. 27, no. 22, pp. 7549–7558, 2015.

[17] M. D. Bhatt and J. Y. Lee, "Advancement of platinum (Pt)-Free (non-Pt precious metals) and/or metal-free (non-precious-metals) electrocatalysts in energy applications: a review and perspectives," *Energy & Fuels*, vol. 34, no. 6, pp. 6634–6695, 2020.

[18] M.-I. Jamesh and M. Harb, "Tuning the electronic structure of the earth-abundant electrocatalysts for oxygen evolution reaction (OER) to achieve efficient alkaline water splitting-a review," *Journal of Energy Chemistry*, vol. 56, pp. 299–342, 2021.

[19] M. Kuang and G. Zheng, "Nanostructured bifunctional redox electrocatalysts," *Small*, vol. 12, no. 41, pp. 5656–5675, 2016.

[20] V. F. Puntes, K. Krishnan, and A. P. Alivisatos, "Synthesis of colloidal cobalt nanoparticles with controlled size and shapes," *Topics in Catalysis*, vol. 19, no. 2, pp. 145–148, 2002.

[21] J. Mosayebi, M. Kiyasatfar, and S. Laurent, "Synthesis, functionalization, and design of magnetic nanoparticles for theranostic applications," *Advanced Healthcare Materials*, vol. 6, no. 23, p. 1700306, 2017.

[22] H. Cheng, N. Yang, Q. Lu, Z. Zhang, and H. Zhang, "Syntheses and properties of metal nanomaterials with novel crystal phases," *Advanced Materials*, vol. 30, no. 26, p. 1707189, 2018.

[23] V. Mantella, L. Castilla-Amorós, and R. Buonsanti, "Shaping non-noble metal nanocrystals via colloidal chemistry," *Chemical Science*, vol. 11, no. 42, pp. 11394–11403, 2020.

[24] Z. G. Wu, M. Munoz, and O. Montero, "The synthesis of nickel nanoparticles by hydrazine reduction," *Advanced Powder Technology*, vol. 21, no. 2, pp. 165–168, 2010.

[25] V. Kandathil, R. B. Dateer, B. S. Sasidhar, S. A. Patil, and S. A. Patil, "Green synthesis of palladium nanoparticles: applications in aryl halide cyanation and hiyama cross-coupling reaction under ligand free conditions," *Catalysis Letters*, vol. 148, no. 6, pp. 1562–1578, 2018.

[26] M. Irfan, R. Rehman, M. R. Razali, R. Shafiq-Ur-Rehman, R. Ateeq-Ur-Rehman, and M. A. Iqbal, "Organotellurium compounds: an overview of synthetic methodologies," *Reviews in Inorganic Chemistry*, vol. 40, no. 4, pp. 193–232, 2020.

[27] V. Gutknecht, B. Walther, H. Noei et al., "Durability of colloidally stabilized supported nickel and nickel platinum nanoparticles during redox-cycling," *Journal of Physical Chemistry C*, vol. 125, no. 15, pp. 8224–8235, 2021.

[28] C. J. Murphy, "Nanocubes and nanoboxes," *Science*, vol. 298, no. 5601, pp. 2139–2141, 2002.

[29] A. J. Ahamed and P. V. Kumar, "Synthesis and characterization of monodisperse Fe-Co-Ni colloidal nanoparticles by polyol method," *J. Environ. Nanotechnol*, vol. 2, no. 2, pp. 76–80, 2013.

[30] D. D. Slave, L. N. Gales, and E. E. Totu, "Applicability of ferromagnetic nanoparticles in surface water treatment with biological loads," *Revista de Chimie*, vol. 67, no. 6, pp. 1034–1038, 2016.

[31] K. Belhamel, H. Kheraz, R. Ludwig, T. K. D. Nguen, N. Allsop, and S. S. Al-Juaid, "Electrodeposition and morphology analysis of nickel nanoparticles from sulphate bath," *E-Journal of Surface Science and Nanotechnology*, vol. 8, pp. 227–232, 2010.

[32] F. B. Susetyo, M. C. Fajrah, and B. Soegijono, "Effect of electrolyte temperature on properties of nickel film coated onto copper alloy fabricated by electroplating," *E-Journal of Surface Science and Nanotechnology*, vol. 18, pp. 223–230, 2020.

[33] Y.-P. Sun, H. W. Rollins, and R. Guduru, "Preparations of nickel, cobalt, and iron nanoparticles through the rapid expansion of supercritical fluid solutions (RESS) and chemical reduction," *Chemistry of Materials*, vol. 11, no. 1, pp. 7–9, 1999.

[34] D. A. Brewster, Y. Bian, and K. E. Knowles, "Direct solvothermal synthesis of phase-pure colloidal NiO nanocrystals," *Chemistry of Materials*, vol. 32, no. 5, pp. 2004–2013, 2020.

[35] M. Trad, A. Nominé, C. Noël, J. Ghanbaja, M. Tabbal, and T. Belmonte, "Evidence of alloy formation in CoNi nanoparticles synthesized by nanosecond-pulsed discharges in liquid nitrogen," *Plasma Processes and Polymers*, vol. 17, no. 5, p. 1900255, 2020.

[36] J. Chaudhary, G. Tailor, D. Verma, and R. Verma, "Synthesis and characterization of cobalt nanocomposite using aniline-formaldehyde resin," *Composites Communications*, vol. 18, pp. 13–18, 2020.

[37] H. N. Abid, U. M. Nayef, and F. A. H. Mutlak, "Preparation and characterization Co3O4 nanoparticles on porous silicon for humidity sensor by photoluminescence," *Optik*, vol. 178, pp. 379–383, 2019.

[38] S. A. Salman, T. Usami, K. Kuroda, and M. Okido, "Synthesis and characterization of cobalt nanoparticles using hydrazine and citric acid," *Journal of Nanotechnology*, vol. 2014, Article ID 525193, 6 pages, 2014.

[39] M. Kawamori, S. Yagi, and E. Matsubara, "Electrochemical analysis in fabrication of Co-Ni alloy nanoparticles in non-aqueous solution," *Journal of MMIJ*, vol. 127, no. 2, pp. 103–107, 2011.

[40] O. Gylienė, M. Šalkauskas, and R. Juškėnas, "The use of organic acids as precipitants for metal recovery from galvanic solutions," *Journal of Chemical Technology and Biotechnology*, vol. 70, no. 1, pp. 111–115, 1997.

[41] J. Qian, X. Zhu, Y. Tao, Y. Zhou, X. He, and D. Li, ""Promotion of Ni2+ removal by masking toxicity to sulfate-reducing bacteria: addition of citrate," (in eng)," *International Journal of Molecular Sciences*, vol. 16, no. 4, pp. 7932–7943, 2015.